

1 **Potential short-term losses of N₂O and N₂ from high**
2 **concentrations of biogas digestate in arable soils**

3 Sebastian Rainer Fiedler¹, Jürgen Augustin², Nicole Wrage-Mönnig¹, Gerald Jurasinski¹,
4 Bertram Gusovius², Stephan Glatzel^{1,*}

5 ¹Faculty of Agricultural and Environmental Sciences, University of Rostock, Rostock, 18059, Germany

6 ²Institute for Landscape Biogeochemistry, Leibniz Centre for Agriculture Landscape Research (ZALF) e.V.,
7 Müncheberg, 15374, Germany

8 *now at: Department of Geography and Regional Research, University of Vienna, Vienna, 1010, Austria

9 *Correspondence to:* S. R. Fiedler (sebastian.fiedler@uni-rostock.de)

10 **Abstract.** Biogas digestate (BD) is increasingly used as organic fertiliser, but has a high potential for NH₃ losses.
11 Its proposed injection into soils as a counter-measure has been suggested to promote the generation of N₂O, leading
12 to a potential trade-off. Furthermore, the effect of high nutrient concentrations on N₂ losses as they may appear
13 after injection of BD into soil has not yet been evaluated. Hence, we performed an incubation experiment with soil
14 cores in a helium-oxygen atmosphere to examine the influence of soil substrate (loamy sand, clayey silt), water-
15 filled pore space (WFPS; 35, 55, 75%) and application rate (0, 17.6 and 35.2 mL BD per soil core [250 cm³]) on
16 the emission of N₂O, N₂ and CO₂ after the usage of high loads of BD. To determine the potential capacity for
17 gaseous losses, we applied anaerobic conditions by purging with helium for the last 24 h of incubation. Immediate
18 N₂O and N₂ emissions as well as the N₂/(N₂O+N₂) ratio depended on soil type and increased with WFPS indicating
19 a crucial role of soil gas diffusivity for the formation and emission of nitrogenous gases in agricultural soils.
20 However, emissions did not increase with the application rate of BD. This is probably due to an inhibitory effect
21 of the high NH₄⁺ content in BD on nitrification. Our results suggest a larger potential for N₂O formation
22 immediately following BD injection in the fine-textured clayey silt compared to coarse loamy sand. By contrast,
23 the loamy sand showed a higher potential for N₂ production under anaerobic conditions. Our results suggest that
24 short-term N losses of N₂O and N₂ after injection may be higher than probable losses of NH₃ following surface
25 application of BD.

26 1 Introduction

27 Nitrous oxide (N₂O) is a potent greenhouse gas (Myhre et al., 2013), with agriculture being its largest single
28 anthropogenic source, contributing about 4.1 Tg N₂O-N yr⁻¹ or 66% of total gross anthropogenic emissions, mainly
29 as a result of mineral nitrogen (N) fertiliser and manure application (Davidson and Kanter, 2014). The generation
30 of nitrogen gas (N₂) is of agronomic interest in terms of nutrient management, since such gaseous losses may imply
31 a significant loss of N from the soil/plant system (Cameron et al., 2013; Friedl et al., 2016). However, from an
32 environmental stance, N₂ is innocuous and, thus, the preferred type of gaseous N-loss from soil (Davidson et al.,
33 2015). In general, the improvement of N use efficiency and thus the decrease of N losses in crop production are
34 paramount in the presence of challenges like food security, environmental degradation and climate change (Zhang
35 et al., 2015).

36 Digestion residues (biogas digestate, BD) from biogas plants are used as organic amendment in agriculture. But,
37 compared to undigested amendments, digestion results in an increased pH, a higher proportion of ammonium
38 (NH₄⁺) and a narrowed carbon (C) / N ratio of BD (Möller and Müller, 2012). These altered chemical properties
39 may promote biochemical reactions in the soil that are responsible for the formation of gaseous N species like
40 N₂O, nitric oxide (NO), N₂ and ammonia (NH₃) (Nkoa, 2013).

41 Significant losses of N as NH₃ may occur within the first hours after manure application (Quakernack et al., 2012).
42 To reduce NH₃ losses, the application of BD by injection is recommended, but this measure can simultaneously
43 increase the potential for N₂O losses compared to surface-application (Velthof and Mosquera, 2011; Wulf et al.,
44 2002). On the one hand, high NH₄⁺ concentrations in the injection band promote nitrification, consuming O₂ and
45 releasing N₂O (Christensen and Rowe, 1984). On the other hand, increased amounts of C in the injection band also
46 promote respiration, additionally depleting O₂ supply (Dell et al., 2011). Altogether, the conditions during the

47 initial phase after injection of BD foster microsites favourable for microbial denitrification, which promote also
48 the formation of N₂ due to anaerobic conditions (Köster et al., 2015; Webb et al., 2010).
49 There is a wealth of biotic and abiotic processes in soils that produce N₂O and N₂, depending on mineral N content,
50 C availability as well as on temperature, most of which are enhanced by anoxic or at least suboxic conditions
51 (Butterbach-Bahl et al., 2013). The amounts and the relative share of N₂ and N₂O in the overall gaseous N
52 emissions depend – among other factors – on the degree of O₂ restriction (Firestone and Davidson, 1989). Soil
53 physical and biotic factors (i.e. diffusion permitted by soil porosity in conjunction with water-filled pore space
54 [WFPS] as well as consumption of O₂ by heterotrophic respiration and nitrification) control the aerobic status of
55 a soil (Ball, 2013; Maag and Vinther, 1999; Uchida et al., 2008). In general, clayey soils exhibit a lower gas
56 diffusivity compared to coarse textured soils. This regularly results in higher denitrification in the former with
57 higher N₂O emission rates, but also a higher probability for the consecutive reduction to N₂ (Ball, 2013; Gu et al.,
58 2013; Senbayram et al., 2014).
59 There is a general lack of knowledge about the effects of high BD concentration on gaseous N-losses as they might
60 appear after injection into soils and their interactions with O₂ limiting factors like soil texture and WFPS, as well
61 as temperature and heterotrophic respiration. Thus, we applied the helium-oxygen (He-O₂) incubation technique
62 (Butterbach-Bahl et al., 2002) in a laboratory experiment to evaluate the effect of the factors suggested above on
63 the emission of N₂O and N₂ from different soils. Simultaneously, CO₂ flux was determined as an indicator for
64 microbial O₂ consumption, O₂ diffusion and also for the degradability of organic C applied with BD (Blagodatsky
65 and Smith, 2012). We hypothesised that (1) N₂O and N₂ emissions will increase with WFPS, (2) gaseous N losses
66 will also be affected by BD application rate, i.e. the hypothetical concentration of C and N resulting from injection,
67 and (3) the clayey silt will induce higher gaseous N losses than the coarse loamy sand.

68 2 Material and Methods

69 2.1 Selected soils, sampling of soil cores and biogas digestate

70 Two soils were selected and both were adjusted to three levels of WFPS and three quantities of BD (Table 1),
71 resulting in 18 factor combinations with three replicates. Temperature was increased from 2 °C during the first
72 two days to 15 °C for the last three days of the incubation. Intact soil cores (diameter 7.2 cm, height 6.1 cm, volume
73 250 cm³) were taken with sample rings in the range from 0–0.10 m depth from two sites with different textures,
74 i.e. sandy loam and clayey silt. The sandy loam samples were collected from a stagnic luvisol (IUSS Working
75 Group WRB, 2006) located in Gülzow (North-East Germany) in the ground moraine of the Weichselian glacial
76 period at 53° 48' 35" N and 12° 4' 20" E. The clayey silt samples were collected from a haplic luvisol located in
77 Dornburg between the foothills and the lowlands of Central Germany at 51° 0' 8" N and 11° 39' 25" E (see Table
78 2 for more details on soil characteristics). After field sampling, the soil cores were dried for 48 h at 40 °C to
79 facilitate adjustment of WFPS.

80 Both sites have been cultivated with similar crop rotations used as feedstock for biogas production and have been
81 amended with biogas digestate for the past nine years. The crop rotation on the sandy loam consisted of maize
82 (*Zea mays* L.), rye (*Secale cereale* L.), sorghum (*Sorghum bicolor* (L.) MOENCH), winter triticale (×
83 *Triticosecale* Wittmack), ryegrass (*Lolium perenne* L.) and winter wheat (*Triticum aestivum* L.). The only

84 difference in the crop rotation on the clayey silt was the cultivation of sudan grass (*Sorghum × drummondii*)
85 instead of sorghum.

86 The biogas digestate used for the incubation was obtained from a biogas plant at 'Gut Dalwitz', an organic farm
87 in northeast Germany. The feedstock for the anaerobic fermentation in the plant consisted of 60 % maize, 20 %
88 solid cattle manure, 10 % dry chicken manure and 10 % rye. The digestate was analysed by LUFA Rostock,
89 Germany and had a pH of 8.3, 2.91% organic C, 0.16% dissolved organic C (DOC), 0.54% N and 0.27% NH₄-N
90 in undried material with a dry matter content of 9.4%.

91 **2.2 Adjustment of WFPS and addition of N**

92 For adjustment of WFPS, the dry and undisturbed soil cores were moistened dropwise. The respective quantities
93 of water were calculated based on the bulk density, an assumed particle density of 2.65 g cm⁻¹ and reduced by the
94 expected moisture input from subsequent addition of BD. The soil cores were then mixed with BD and finally
95 repacked to reach nutrient concentrations comparable to that in injection bands. The amounts of added BD were
96 calculated with an assumed injection of 160 kg N ha⁻¹ into soil with row spaces of 0.15 m (narrow injection bands
97 with low BD concentration, LOBD) and 0.30 m (wide injection bands with high BD concentration, HIBD). These
98 are common ranges used by injection machinery and correspond to 17.6 and 25.3 mL BD per sample ring. After
99 this procedure, the soil cores were sealed with plastic lids and stored immediately at 2 °C until the beginning of
100 the incubation within a week.

101 **2.3 Determination of gas fluxes**

102 The measurements of N₂, N₂O and CO₂ fluxes were applied following the He-O₂ method (Butterbach-Bahl et al.,
103 2002; Scholefield et al., 1997). Six soil cores (i.e. the repetitions of two factor combinations at a time, Table 3)
104 were placed simultaneously in special gas-tight incubation vessels inside a climate chamber. Analyses were
105 conducted in the laboratory of the Institute for Landscape Biogeochemistry, Leibniz Centre for Agricultural
106 Landscape Research (ZALF), Müncheberg, Germany. Before flux measurements, the vessels were evacuated to
107 0.047 bar and flushed with an artificial He/O₂ gas mixture (20.49 % O₂, 345.5 ppm CO₂, 359 ppb N₂O, 1863 ppb
108 CH₄, 2.46 ppm N₂, rest He) four times consecutively to remove ambient N₂. Subsequently, the air temperature of
109 the climate chamber was set to 2 °C and a continuous He/O₂ gas flow rate of 15 ml min⁻¹ was applied to the vessel
110 headspace for 72 h to remove residues of N₂ from soil cores by diffusion, including a restricted N₂ production by
111 decreased microbial activity. After this pre-incubation in the following two days the headspace concentration of
112 N₂O and CO₂ was measured once daily in the morning. To compensate for the lower precision of the detector for
113 N₂ in relation to the detector for N₂O and CO₂ (Eickenscheidt et al., 2014), N₂ concentrations were measured
114 consecutively three times daily in the morning. Immediately after the last measurement on the second day, the
115 temperature was set to 15 °C and the measurements were continued for another two days. Finally, the He/O₂ gas
116 mixture was substituted by pure He and, following 24 h of acclimatisation, gas measurements were carried out
117 once again (Figure 1) to determine the generation of N₂O and N₂ in a completely anaerobic soil matrix. The latter
118 step is important to get a clue about the actual potential for gaseous N losses after highly concentrated BD
119 application. The settings of the chromatographs for gas analyses are described in Eickenscheidt et al. (2014). Gas
120 fluxes were calculated according to Eq. (1):

$$f = \frac{M \times p \times v \times dc}{R \times T \times A}, \quad (1)$$

where f is the flux (N_2 and CO_2 : $\text{mg m}^{-2} \text{h}^{-1}$, N_2O : $\mu\text{g m}^{-2} \text{h}^{-1}$), M the molar mass in g mol^{-1} (N_2 : 28, CO_2 : 44, N_2O : 44), p the air pressure (Pa), v the air flow (L h^{-1}), R the gas constant ($8.31 \text{ J mol}^{-1} \text{ K}^{-1}$), T the temperature inside the chamber (K), A the area of the incubation vessel (m^2), and dc the difference of gas concentrations (N_2 and CO_2 : ppm, N_2O : ppb) between inlet and outlet of a vessel.

To enhance the tightness against atmospheric N_2 contamination, the lids of the incubation vessels were permanently purged with helium. We obtained blank values by inserting aluminium blocks into the vessels before each measurement cycle. Since this blank values were usually steady with means of 1.9 ($1\sigma = 0.9$) ppm N_2 , 349.6 ($1\sigma = 11.4$) ppb N_2O and 353.9 ($1\sigma = 13.5$) ppm CO_2 , we suggest that the vessels were tight. Derived from the blank values, lowest detectable fluxes were on average 0.427 ($1\sigma = 0.271$) $\text{mg N}_2\text{-N m}^{-2} \text{h}^{-1}$, 3.6 (3.1) $\mu\text{g N}_2\text{O-N m}^{-2} \text{h}^{-1}$ and 0.918 (0.693) $\text{mg CO}_2\text{-C m}^{-2} \text{h}^{-1}$. For flux estimation, the blank values were subtracted from the values measured at the respective outlet. Estimated fluxes from the soil cores smaller than the respective blank fluxes of each day were set to zero.

134

135 2.4 Soil analyses after incubation

136 After incubation, the soil cores were stored at 2 °C until they were extracted with 0.1 M KCl solution (soil to extract
137 ratio 1:4, standardised extraction method of the commissioned laboratory at Leibniz Centre for Agricultural
138 Landscape Research e. V.) and analysed for NH_4^+ and nitrate (NO_3^-) by spectrophotometry according to DIN ISO
139 14256 with a continuous flow analyser ‘CFA-SAN’, Skalar Analytical B.V., the Netherlands and for DOC by
140 combustion according to DIN ISO 10694 with an analyser ‘RC 612’, Leco Instruments GmbH, Germany.

141 2.5 Statistical analysis

142 All statistical analyses were done using R version 3.2.3 (R Core Team, 2015) with the data of the measuring days
143 under He- O_2 atmosphere. Data from the vessels with the factor combination of 35% WFPS and LOBD with clayey
144 silt were omitted due to technical reasons during sample preparation. For the final period of pure He headspace,
145 some gas concentration data could not be documented. For loamy sand, this affects all WFPS levels with LOBD
146 (N_2 and N_2O), the treatment 75% WFPS with 320 kg N h^{-1} (N_2O and CO_2) and for the clayey silt the treatment
147 35% WFPS without amendment (N_2O and CO_2).

148 To account for repeated measurement of vessels, linear mixed effect models were applied with package ‘lmerTest’
149 version 2.0-33 (Kuznetsova et al., 2016) for fluxes of each gas type. The three pseudo-replicated fluxes from the
150 N_2 measurements of each vessel were averaged for each day to obtain the same number of observations as for N_2O
151 and CO_2 fluxes. The fixed structure of models included soil type, WFPS, amount of digestate, temperature, NO_3^-
152 and DOC contents after incubation as well as the fluxes of N_2O (in the model for N_2) and CO_2 (in the models for
153 N_2 , N_2O and $\text{N}_2/[\text{N}_2+\text{N}_2\text{O}]$ product ratio). Soil NH_4^+ was omitted since it showed high autocorrelation with the
154 amount of BD applied. The individual soil cores in the vessels were set as random effect (nested within the week
155 of incubation and with allowance for a variable slope of the effect each day) with regard to lack of independence
156 of consecutive measurements. The model responses for N_2 , N_2O and CO_2 were log transformed ($\ln[\text{value} + 1]$)

157 since gas fluxes from soils usually show lognormal distributions (Kaiser et al., 1998). The function ‘step’ was used
158 for automatic backward selection of models based on AIC (Akaike’s ‘An Information Criterion’). The skewness
159 (γ) was calculated with R package ‘moments’ version 0.14 (Komsta and Novomestky, 2015) to check residuals
160 for normal distribution and $|\gamma| \leq 2$ was assumed as appropriate (West et al., 1995). For mixed effects models, p -
161 values of the ANOVA (type 2) were calculated based on Satterthwaite’s approximation)
162 Cumulated gas fluxes were estimated with a bootstrap method using function ‘auc.mc’ of R package ‘flux’ version
163 0.3-0 (Juraski et al., 2014) for the R statistical software version 3.2.3 (R Core Team, 2015). In short, the fluxes
164 for the period of aerobic headspace were cumulated in 100 iterations, while for each run two fluxes were omitted
165 randomly. Then, the resulting data were used to calculate means and standard deviations.

166 **3 Results**

167 **3.1 Soil NH₄⁺, NO₃⁻ and DOC contents**

168 The calculated application of NH₄⁺-N from BD per kg soil approximated for the sandy loam 247.0 mg (LOBD)
169 and 494.0 mg (HIBD), and for the clayey silt 266.0 mg (LOBD) and 532.0 mg (HIBD). The NO₃⁻ content of BD
170 was negligible. In general, the NH₄⁺ content of the soils after incubation increased with digestate application with
171 lower amounts detected in the clayey silt. Nitrate was found almost exclusively in the latter soil. (Fig. 2).
172 The amounts of measured DOC increased with the application rate of BD, but with higher magnitudes for the
173 loamy sand than for the clayey silt (Table 4).

174 **3.2 CO₂ fluxes**

175 CO₂ fluxes showed clear differences between the soils: under all combinations of temperature and oxygen, the
176 fluxes were always larger from loamy sand compared to clayey silt (Table A1). In general, mean fluxes from
177 loamy sand increased with the amount of digestate during each of the different periods regarding temperature and
178 headspace aerobicity, but showed no obvious pattern with WFPS. There was no clear trend of fluxes with the
179 amount of amendment, but a slight trend of decreasing fluxes with increasing WFPS for the clayey silt. However,
180 the predictive power of WFPS on CO₂-C fluxes was minor since it was eliminated during stepwise regression
181 fitting. By contrast, soil type, amount of digestate, temperature as well as the DOC content after the incubation
182 had significant ($p < 0.01$) effects (Table 5).

183 **3.3 N₂O fluxes**

184 The mean N₂O fluxes from the loamy sand in the He-O₂ headspace were virtually zero, independent of temperature
185 and WFPS as well as the amount of BD application (Fig. 3, Table A2). In contrast, the emissions of the clayey silt
186 increased with temperature and were highest at 15 °C with intermediate WFPS and amount of BD, i.e. 6.2 mg
187 N₂O-N m⁻² h⁻¹ at 55% with LOBD, respectively. Surprisingly, at 15 °C, increasing the amount of BD up to HIBD
188 did not increase the observed N₂O efflux; rather it decreased the efflux significantly ($p < 0.05$, Tuckey’s HSD) at
189 55% and also, but not significantly, at 75% WFPS (Fig. 3, Table A2). According to the linear mixed model for

190 N₂O fluxes in aerobic conditions, WFPS, amount of digestate, temperature, DOC content of soil after incubation
191 and CO₂ fluxes had significant ($p < 0.001$) effects on N₂O flux (Table 5).

192 Under anaerobic headspace conditions, the overall highest mean N₂O flux was observed from the clayey silt at
193 35% WFPS with HIBD (11.7 mg N₂O-N m⁻² h⁻¹). The same soil showed a tendency of decreasing N₂O fluxes with
194 increasing WFPS and amendment. In the loamy sand, the pure He-atmosphere induced increasing mean N₂O fluxes
195 (up to 1.3 mg N₂O-N m⁻² h⁻¹) with increasing WFPS (Fig. 3, Table A2). Thus, the anaerobic headspace induced a
196 change only in the loamy sand by increasing emissions.

197 **3.4 N₂ fluxes**

198 From the loamy sand, no or only small rates of N₂ were detected at both temperatures under He-O₂ atmosphere
199 (Fig. 4, Table A3). The clayey silt showed mean fluxes of up to 1.4 mg N₂ m⁻² h⁻¹ at 2 °C (all incubations with
200 75% WFPS) and up to 3.8 mg N₂ m⁻² h⁻¹ at 15 °C (75% WFPS with LOBD), but no fluxes in all BD treatments
201 with 35% WFPS. Put simply, temperature had a small effect on N₂ emissions from the sandy loam with no
202 consistent influence of WFPS and the amount of BD. In contrast, the clayey silt emitted increasing fluxes with
203 increasing temperature and WFPS. However, the application rise from LOBD up to HIBD at 15 °C resulted in
204 slightly, but not significantly ($p > 0.05$, Tuckey's HSD) decreased fluxes (Fig. 4, Table A3). The summary of the
205 linear mixed model for N₂ fluxes under aerobic conditions revealed significant effects ($p < 0.05$) of soil type,
206 WFPS, the amount of digestate, temperature, DOC content after incubation and N₂O flux (Table 5).

207 After switching the atmosphere to pure He, the N₂ fluxes from the sandy loam increased more than 60-fold. In
208 contrast to aerobic conditions, all measured factor combinations showed mean fluxes up to 35.1 mg N₂ m⁻² h⁻¹
209 (55% with 320 kg N ha⁻¹) (Fig. 2, Day 5 in Table A3). Mean fluxes from clayey silt increased only up to 9.3 mg
210 N₂ m⁻² h⁻¹ in amended treatments. Thus, the loamy sand exhibited a much more intense reaction under anaerobic
211 headspace conditions.

212 **3.5 N₂/(N₂ + N₂O-N) product ratio**

213 No clear trend of the product ratio of N₂/(N₂ + N₂O-N) was found for incubations of the loamy sand. However,
214 there was a clear distinction of the ratios for this soil under aerobic and anaerobic atmospheres: while the ratios
215 were close to zero in the former, they were close to one in the latter (Fig. 5). In contrast, in the clayey silt the ratios
216 increased with WFPS and were affected by digestate amendment under both the aerobic and the anaerobic
217 atmospheres, where the highest ratios (up to 0.8) were found in treatments without digestate and at least 55%
218 WFPS. The digestate-amended treatments showed ratios around or above 0.5, with exception of the 35% WFPS
219 treatments, which had ratios close to zero. According to the linear mixed model, the product ratio under aerobic
220 conditions was affected significantly ($p < 0.01$) by soil type and the amount of digestate (Table 5).

221 4 Discussion

222 4.1 Increased BD application rate did not increase N₂O and N₂ losses probably due to inhibitory effect 223 of high NH₄⁺ concentrations

224 The overall N₂O fluxes corresponded well with those from other studies with similar incubation conditions and
225 application rates of BD in terms of N ha⁻¹ (Köster et al., 2015; Senbayram et al., 2012; Severin et al., 2015).
226 However, the latter studies assumed a distribution of BD into soil by a cultivator, which implies a smaller
227 concentration of BD than we actually applied. Although we observed differences in N₂O emissions between soils,
228 soil type was not confirmed as a significant effect. Nevertheless, WFPS and temperature, which are well known
229 controls of N₂O generation (Maag and Vinther, 1999), showed significant influences. Both are physical (by gas
230 diffusion) and biological (by increased metabolic activity and consequently increased O₂ consumption by
231 respiration) drivers for O₂ availability (Ball, 2013; Maag and Vinther, 1999). Accordingly, CO₂ flux (resulting
232 from respiration of O₂) generally increased with temperature and was also identified as significant by regression
233 selection.

234 The mean N₂ fluxes of up to 0.5 (loamy sand) and 3.8 mg N m⁻² h⁻¹ (clayey silt) at 15° C (Fig. 5, Table A3) were
235 considerably smaller than the mean fluxes of up to 13.0 mg m⁻² h⁻¹ observed by Köster et al. (2015) during the first
236 five days of their incubation. Although the amount of BD in terms of applied N (250 kg ha⁻¹) was comparable,
237 Köster et al. (2015) used a higher WFPS of 90%, which may have increased the generation of N₂. In contrast to
238 N₂O emission rates, the observed N₂ fluxes depended not only on WFPS, but also on soil type (Table 5). This is
239 most likely due to the direct influence of soil structure on diffusivity and the resulting supply with O₂ (Balaine et
240 al., 2016; Butterbach-Bahl et al., 2013). N₂O flux showed also a significant effect during regression selection for
241 N₂. N₂O is the direct precursor of N₂ in denitrification, so the flux of the latter depends on the availability of the
242 former. However, temperature showed no significant effect.

243 N₂/(N₂+N₂O) ratios were significantly determined only by soil type and WFPS: while no clear trend was
244 observable for the loamy sand, there was a pronounced effect in the clayey silt (Fig 4). We attribute the lack of a
245 trend in loamy sand to generally adverse conditions for the formation of N₂O and N₂, i.e. a sufficient supply of O₂
246 (see section 4.2). Contrary, the influence of WFPS apparently mirrored favourable conditions in the clayey silt
247 (Table 5). Simultaneously, with increasing WFPS, the reduction of N₂O as an alternative electron acceptor under
248 reduced O₂ supply accelerates (Tiedje, 1988). Accordingly, no or rather small fluxes of the investigated gaseous
249 N species were generally found in our presumably well aerated treatments with 35% WFPS.

250 In our study, one treatment (clayey silt, 55% WFPS, LOBD) showed exceptionally large mean N₂O fluxes of up
251 to 7.1 mg N m⁻² h⁻¹ (Fig. 3, Table A2). This could be evidence that the injection of such commonly applied amounts
252 of BD-N (i.e., 160 kg N ha⁻¹) may favour much larger losses of N₂O compared to an even distribution of BD in a
253 soil surface due to larger substrate concentration in injection slits. However, with higher amendments (i.e. HIBD),
254 we observed partially significant ($p < 0.05$, Tuckey's HSD) reductions of N₂O and a decreasing tendency of N₂
255 emissions (Table A2, Table A3). In line with this, the amount of BD showed a significant effect during the
256 regression selection on N₂O, but not on N₂ fluxes (Table 5). A coherent reasoning for the rather smaller emissions
257 of highly amended HIBD treatments might lie in an inhibitory effect of NH₃ on nitrification. Accordingly,
258 Anthonisen et al. (1976) found an inhibition of nitrification in the presence of 0.1 to 150 mg NH₃ L⁻¹. The

259 application rate in the treatments with HIBD amounted to ca. 500 mg NH₄⁺-N (kg soil)⁻¹ (Fig. 3) which corresponds
260 to 25.8 mg NH₃-N (kg soil)⁻¹ at 15 °C when applying the pH of the BD and assuming all extractable NH₄⁺-N to be
261 in solution (Emerson et al., 1975). Hence, we consider this inhibitory effect as the reason for the missing increase
262 of N₂O and N₂. Additionally, due to the increased pH of BD (Möller and Müller, 2012), the amount of NH₄⁺ fixed
263 as NH₃ by soil organic matter increases and, moreover, this fixed NH₃ is not readily extractable by the KCl method
264 we have applied (Kissel et al., 2008). This is consistent with the observation of generally higher N₂O and N₂ fluxes
265 from the clayey silt since clay increases the sorption capacity of soils for NH₄⁺, thus reducing the inhibitory effect
266 on nitrification (Kissel et al., 2008). However, because we mixed the BD with the soil, one would expect a lower
267 NH₃ fixation in tubular injection slits *in situ*, resulting in probably lower N₂O and N₂ fluxes from clayey soils.
268 High NH₄⁺ loads in conjunction with an increased pH favour NO₂⁻ accumulation because NO₂⁻ oxidising bacteria
269 are less resilient against high concentrations of NH₃ than NH₃ oxidising bacteria (Anthonisen et al., 1976). This
270 NO₂⁻ should have protonated then partly to toxic and unstable HNO₂, which drives biological and chemical
271 production of NO and N₂O for detoxification (Venterea et al., 2015). Although we did not determine NO₂⁻, we
272 suggest a dominant role of nitrifier denitrification, i.e., NO₂⁻ reduction, in the generation of N₂O during our
273 experiment, especially during the anaerobic headspace conditions at the end of the incubation, resulting in the
274 relatively small NO₃⁻ recovery in both soils. Accordingly, coupled nitrification-denitrification and bacterial
275 denitrification have been found to dominate the production of N₂O directly after application of BD (Köster et al.,
276 2011; Senbayram et al., 2009). However, N₂O-N losses were clearly larger than N₂ losses under aerobic headspace
277 in the clayey silt. This indicates that much of the N gas loss was driven by processes other than canonical
278 denitrification. Under the above mentioned conditions, NO-N losses may exceed N₂O losses (Venterea et al.,
279 2015), calling for taking account of NO measurements in future studies.

280 Supposed that 15 % of NH₄⁺-N is volatilised as NH₃ within the first ten hours after surface application of BD
281 (Quakernack et al., 2012), the losses from the NH₄⁺ amounts we applied would averaged to 80 mg NH₃-N m⁻² h⁻¹
282 (LOBD) and 160 mg NH₃-N m⁻² h⁻¹ (HIBD). The actual losses of up to 11.7 mg N₂O-N m⁻² h⁻¹ at 30 % WFPS in
283 the clayey soil (Table A2) or of up to 35.1 mg N₂ m⁻² h⁻¹ at 55 % WFPS in the sandy loam (Table A3) from our
284 HIBD treatments add up to 117 mg N₂O-N and 351 mg N₂, respectively, for the same period. Hence, increased
285 N₂O and N₂ emissions following injection of BD might effectively cause higher N losses compared to a surface
286 application and deserve closer attention in future.

287 4.2 Different effects of soil diffusivity on N₂O and N₂ fluxes

288 Apparently, the tested factors affected the N₂O and N₂ fluxes from both soils in a different way. A specific soil
289 characteristic that exhibits such a fundamental control on biogeochemical processes such as denitrification is the
290 diffusivity for O₂ (Ball, 2013; Letey et al., 1980; Parkin and Tiedje, 1984), which is a main soil characteristic
291 responsible for the appearance of anaerobic microsites. In general, diffusivity integrates the soil porosity, i.e., pore
292 continuity and size as well as WFPS, which control both soil N₂O and N₂ emissions (Balaine et al., 2016; Ball,
293 2013; Letey et al., 1980). Soils with a coarser texture like the loamy sand have a higher proportion of macropores
294 and thus a higher gas diffusion compared with fine textured soils like the clayey silt we used (Groffman and Tiedje,
295 1991). This lets us expect conditions that are more favourable for N₂O and N₂ generation in the latter due to
296 relatively poor diffusion characteristics and, thus, a smaller O₂ supply. Actually, although we incubated the soils

297 at comparable levels of WFPS and BD amendments, the apparent lower diffusivity led to larger N₂O and N₂
298 production in the treatments with the clayey silt in relation to the loamy sand.

299 The role of the distinct diffusivities of both soils is corroborated by our observations of the gas fluxes in anaerobic
300 headspace. With switching the He-O₂ atmosphere in the headspace to pure He, the denitrification potential can be
301 tested because anaerobicity eliminates respiration processes that use O₂ as electron acceptor (Parkin and Tiedje,
302 1984). We acknowledge e.g. DNRA and anammox as possible additional sources of N₂O and N₂ under such
303 conditions but we were not able to quantify their contribution. The anaerobic headspace induced a considerable
304 increase of N₂O fluxes in the loamy sand, but not in the clayey silt. Concurrently, the N₂ fluxes increased in both
305 soils, but pronounced, i.e. more than 60-fold, in the sandy loam. These observed changes resulting from oxygen
306 deprivation imply that, during the previous aerobic conditions, the diffusivity of the sandy loam was too high to
307 allow for a sufficient establishment of anaerobic microsites while the clayey silt ensured a moderate diffusional
308 constraint to maintain suboxic conditions. In general, only N₂O fluxes from treatments with negligible fluxes
309 during the previous aerobic period increased under anaerobic conditions, including all treatments with loamy sand
310 (Fig. 3, Table A2). At the same time, there was a reduction of N₂O fluxes in most clayey silt treatments. However,
311 a closer look reveals that virtually all of the latter treatments showed increased N₂ flux rates. Hence, there was an
312 enhanced reduction of N₂O to N₂, which is reflected in the increased N₂/(N₂ + N₂O) ratio (Fig. 5) and points to
313 intensified reduction of N₂O due to the lack of oxygen (Parkin and Tiedje, 1984). The much larger N₂ fluxes from
314 the loamy sand compared to the clayey silt might have been caused as well by poor NO₃⁻ availability (Fig. 2) and
315 a high availability of C (Table 4), which promoted the reduction of N₂O to N₂ (Senbayram et al., 2012). Further,
316 we found no evidence for any shortage of substrate in the clayey silt during the subsequent anaerobic headspace
317 conditions. However, the cumulated fluxes of both N₂ and N₂O amounted to a maximum absolute loss of 9.4 (1σ
318 = 0.3) mg N per kg soil in the clayey silt with LOBD and 55% WFPS, which was roughly 3.5% of the calculated
319 NH₄⁺-N applied with BD (Fig. 2). On the other hand, the N₂/(N₂+N₂O) ratios increased only slightly (Fig. 5) and,
320 in contrast to the loamy sand, there were still significant N₂O fluxes in the clayey silt (Fig. 3). This points to still
321 sufficient stocks of NO₃⁻ in the latter (Senbayram et al., 2012). In fact, the NO₃⁻ stock was greater in the clayey silt
322 than in loamy sand after incubation (Fig. 2). Thus, we suggest that the gas fluxes were unaffected by the change
323 to anaerobic headspace in the clayey silt due to already low O₂ concentrations as a result of poor diffusivity. In
324 conclusion, distinct gas diffusivities of both soils can be proposed as the main reason for the differing N₂O and N₂
325 fluxes.

326 In interaction with soil diffusivity, respiration affects the aerobicity of a soil matrix by concurrent consumption
327 and formation of O₂ and CO₂ as well. Depending on microbial C availability, respiration could be indicated by
328 DOC, though not all DOC might be readily degradable (Cook and Allan, 1992). Generally, DOC content after our
329 incubation increased with application rate of BD (Table 4), but DOC content was always smaller in clayey silt.
330 This might reflect a stronger sorption of C and thus a lower availability for respiration in the clayey silt compared
331 to loamy sand (Kaiser and Guggenberger, 2000). If we compare DOC concentrations with cumulated flux rates of
332 CO₂ over the period of aerobic headspace, we find a good regression fit ($R^2 = 0.91$, $p < 0.001$) for both soils (Fig.
333 6) indicating a sufficient availability of C from BD for respiration and, thus, implicitly also for denitrification
334 (Reddy et al., 1982). Moreover, as increased DOC enhanced respiration (Table A1), it consequently affected O₂
335 consumption and, thus, also the emergence of anaerobic microsites (Azam et al., 2002). Accordingly, there is also

336 a good correlation between cumulated CO₂ and N₂O + N₂ fluxes for the same period from the clayey silt ($R^2 =$
337 0.93, $p = 0.001$), when the treatments with 35 % WFPS (which showed virtually no N emissions) are omitted (Fig.
338 7). However, there was no such a correlation for the loamy sand. This confirms the interactive effect of diffusivity
339 (induced by both the soils and WFPS) and C availability on the emissions of N₂O and N₂, which, nevertheless,
340 interacted with the inhibitory effect of high NH₄⁺ loads on nitrification (see chapter 4.1).

341 **5 Relevance and implications**

342 Our aim was to estimate the effect of differing soil environmental conditions on gaseous N losses – and not to
343 draw conclusions about the long-term dynamics of N₂ and N₂O emissions after BD application in concentrations
344 similar to injection. In another laboratory study at a WFPS of 65%, Senbayram et al. (2009) measured only one
345 peak within two days without a repeated increase later, regardless the amount of applied BD. Thus, we assume a
346 single peak shortly after application holds also true for our incubation. We assume also the measurements after
347 only 24 hours of anaerobicity in the headspace to be representative for the emission potential since Wang et al.
348 (2011; 2013) showed in similar studies that the emission of N₂ and N₂O peaked within less than 24 hours after
349 switching their headspace from aerobic to anaerobic conditions.

350 **In summary**, as hypothesised, N₂O and N₂ emissions as well as the N₂/(N₂O+N₂) ratio increased with WFPS, most
351 probably due to restricted supply of O₂. Contrary to our second hypothesis, the gaseous losses of N₂O and N₂ did
352 not increase with the application rate of BD. This indicates an inhibitory effect of high NH₃ and NH₄⁺
353 concentrations on nitrification, which are found typically in BD. **At the same time**, the N₂/(N₂O+N₂) ratio tended
354 to decrease with application rate as supposed, probably due to a copious supply with NO₂⁻ and NO₃⁻ from oxidised
355 BD-NH₄⁺. Confirming our third hypothesis, the fine textured clayey silt induced larger gaseous N losses and a
356 higher N₂/(N₂O+N₂) ratio than the coarse loamy sand by the apparent distinct diffusivities of both soils. Overall,
357 there was a larger potential for formation of N₂O in the fine-textured clayey silt compared to the coarse loamy
358 sand after the application of high concentrations of BD as they may appear after injection. However, the loamy
359 sand showed a large potential for N₂ formation under anaerobic headspace conditions.

360 **Since coupled nitrification-denitrification N losses from injected BD seem to be massive in your study, the short-**
361 **term emissions of N₂O and N₂ after injection appear to offset the reduced NH₃-N losses that would have arose**
362 **hypothetically from surface application.** Further investigations are needed in regarding the dynamics and the
363 duration of the observed effects and their reliability for field conditions.

364 **Acknowledgements**

365 We thank the editor Karsten Kalbitz and three anonymous referees for their careful reading, critical comments and
366 valuable suggestions. We are very grateful to Heinrich Graf von Bassewitz and Matthias Haß from Gut Dalwitz
367 for their straightforward support with substrate from their anaerobic digester. We thank Madlen Pohl from the
368 ZALF, Institute for Landscape Biogeochemistry, Müncheberg, Germany, most sincerely for managing the
369 laboratory analyses of the soil samples. The joint research project underlying this report was funded by the German
370 Federal Ministry of Food and Agriculture under the funding identifier 22007910.

371

372 **References**

- 373 Anthonisen, A. C., Loehr, R. C., Prakasam, T. B. S., and Srinath, E. G.: Inhibition of Nitrification by Ammonia
374 and Nitrous Acid, *J. - Water Pollut. Control Fed.*, 48, 835–852, 1976.
- 375 Azam, F., Müller, C., Weiske, A., Benckiser, G., and Ottow, J.: Nitrification and denitrification as sources of
376 atmospheric nitrous oxide – role of oxidizable carbon and applied nitrogen, *Biol. Fertil. Soils*, 35, 54–61,
377 doi:10.1007/s00374-001-0441-5, 2002.
- 378 Balaine, N., Clough, T. J., Beare, M. H., Thomas, S. M., and Meenken, E. D.: Soil Gas Diffusivity Controls N₂O
379 and N₂ Emissions and their Ratio, *Soil. Sci. Soc. Am J*, 80, 529–540, doi:10.2136/sssaj2015.09.0350, 2016.
- 380 Ball, B. C.: Soil structure and greenhouse gas emissions: a synthesis of 20 years of experimentation, *Eur. J. Soil*
381 *Sci.*, 64, 357–373, doi:10.1111/ejss.12013, 2013.
- 382 Blagodatsky, S. and Smith, P.: Soil physics meets soil biology: Towards better mechanistic prediction of
383 greenhouse gas emissions from soil, *Soil Biol. Biochem.*, 47, 78–92, doi:10.1016/j.soilbio.2011.12.015,
384 2012.
- 385 Butterbach-Bahl, K., Baggs, E. M., Dannenmann, M., Kiese, R., and Zechmeister-Boltenstern, S.: Nitrous oxide
386 emissions from soils: how well do we understand the processes and their controls?, *Philos. Trans. R. Soc., B*,
387 368, doi:10.1098/rstb.2013.0122, 2013.
- 388 Butterbach-Bahl, K., Willibald, G., and Papen, H.: Soil core method for direct simultaneous determination of N₂
389 and N₂O emissions from forest soils, *Plant Soil*, 240, 105–116, doi:10.1023/A:1015870518723, 2002.
- 390 Cameron, K. C., Di, H. J., and Moir, J. L.: Nitrogen losses from the soil/plant system: a review, *Ann. Appl.*
391 *Biol.*, 162, 145–173, doi:10.1111/aab.12014, 2013.
- 392 Christensen, J. P. and Rowe, G. T.: Nitrification and oxygen consumption in northwest Atlantic deep-sea
393 sediments, *J. Mar. Res.*, 42, 1099–1116, doi:10.1357/002224084788520828, 1984.
- 394 Cook, B. D. and Allan, D. L.: Dissolved organic carbon in old field soils: Total amounts as a measure of
395 available resources for soil mineralization, *Soil Biol. Biochem.*, 24, 585–594, doi:10.1016/0038-
396 0717(92)90084-B, 1992.
- 397 Davidson, E. A. and Kanter, D.: Inventories and scenarios of nitrous oxide emissions, *Environ. Res. Lett.*, 9,
398 105012, 2014.
- 399 Davidson, E. A., Suddick, E. C., Rice, C. W., and Prokopy, L. S.: More Food, Low Pollution (Mo Fo Lo Po): A
400 Grand Challenge for the 21st Century, *J. Environ. Qual.*, 44, doi:10.2134/jeq2015.02.0078, 2015.
- 401 Dell, C. J., Meisinger, J. J., and Beegle, D. B.: Subsurface Application of Manures Slurries for Conservation
402 Tillage and Pasture Soils and Their Impact on the Nitrogen Balance, *J. Environ. Qual.*, 40,
403 doi:10.2134/jeq2010.0069, 2011.
- 404 Eickenscheidt, T., Heinichen, J., Augustin, J., Freibauer, A., and Drösler, M.: Nitrogen mineralization and
405 gaseous nitrogen losses from waterlogged and drained organic soils in a black alder (*Alnus glutinosa* (L.)
406 Gaertn.) forest, *Biogeosciences*, 11, 2961–2976, doi:10.5194/bg-11-2961-2014, 2014.
- 407 Emerson, K., Russo, R. C., Lund, R. E., and Thurston, R. V.: Aqueous Ammonia Equilibrium Calculations:
408 Effect of pH and Temperature, *J. Fish. Res. Board Can.*, 32, 2379–2383, doi:10.1139/f75-274, 1975.

409 Firestone, M. K. and Davidson, E. A.: Microbiological basis of NO and N₂O production and consumption in
410 soil, in: Exchange of Trace Gases Between Terrestrial Ecosystems and the Atmosphere, Andreae, M.O. a. S.
411 D.S. (Ed.), Wiley, Chichester, 7–21, 1989.

412 Friedl, J., Scheer, C., Rowlings, D. W., McIntosh, H. V., Strazzabosco, A., Warner, D. I., and Grace, P. R.:
413 Denitrification losses from an intensively managed sub-tropical pasture – Impact of soil moisture on the
414 partitioning of N₂ and N₂O emissions, *Soil Biol. Biochem.*, 92, 58–66, doi:10.1016/j.soilbio.2015.09.016,
415 2016.

416 Groffman, P. M. and Tiedje, J. M.: Relationships between denitrification, CO₂ production and air-filled porosity
417 in soils of different texture and drainage, *Soil Biol. Biochem.*, 23, 299–302, doi:10.1016/0038-
418 0717(91)90067-T, 1991.

419 Gu, J., Nicoullaud, B., Rochette, P., Gossel, A., Hénault, C., Cellier, P., and Richard, G.: A regional experiment
420 suggests that soil texture is a major control of N₂O emissions from tile-drained winter wheat fields during
421 the fertilization period, *Soil Biol. Biochem.*, 60, 134–141, doi:10.1016/j.soilbio.2013.01.029, 2013.

422 Jurasinski, G., Koebsch, F., and Hagemann, U.: flux: Flux rate calculation from dynamic closed chamber
423 measurements, R package version 0.3-0, <https://CRAN.R-project.org/package=flux> (last access: 10 August
424 2017), 2014.

425 Kaiser, E. A., Kohrs, K., Kucke, M., Schnug, E., Heinemeyer, O., and Munch, J. C.: Nitrous oxide release from
426 arable soil: Importance of N-fertilization, crops and temporal variation, *Soil Biol. Biochem.*, 30, 1553–1563,
427 doi:10.1016/S0038-0717(98)00036-4, 1998.

428 Kaiser, K. and Guggenberger, G.: The role of DOM sorption to mineral surfaces in the preservation of organic
429 matter in soils, *Org. Geochem.*, 31, 711–725, doi:10.1016/S0146-6380(00)00046-2, 2000.

430 Kissel, D. E., Cabrera, M. L., and Paramasivam, S.: Ammonium, Ammonia, and Urea Reactions in Soils, in:
431 Nitrogen in Agricultural Systems, Agronomy Monographs, American Society of Agronomy, Crop Science
432 Society of America, Soil Science Society of America, Madison, WI, 101–155, 2008.

433 Komsta, L. and Novomestky, F.: moments: Moments, cumulants, skewness, kurtosis and related tests, R package
434 version 0.14, <https://cran.r-project.org/package=moments> (last access: 10 August 2017), 2015.

435 Köster, J. R., Cárdenas, L., Senbayram, M., Bol, R., Well, R., Butler, M., Mühling, K. H., and Dittert, K.: Rapid
436 shift from denitrification to nitrification in soil after biogas residue application as indicated by nitrous oxide
437 isotopomers, *Soil Biol. Biochem.*, 43, 1671–1677, doi:10.1016/j.soilbio.2011.04.004, 2011.

438 Köster, J. R., Cárdenas, L. M., Bol, R., Lewicka-Szczebak, D., Senbayram, M., Well, R., Giesemann, A., and
439 Dittert, K.: Anaerobic digestates lower N₂O emissions compared to cattle slurry by affecting rate and
440 product stoichiometry of denitrification – An N₂O isotopomer case study, *Soil Biol. Biochem.*, 84, 65–74,
441 doi:10.1016/j.soilbio.2015.01.021, 2015.

442 Kuznetsova, A., Brockhoff, P. B., and Christensen, R. H. B.: lmerTest: Tests in Linear Mixed Effects Models, R
443 package version 2.0-33, <https://cran.r-project.org/package=lmerTest> (last access: 10 August 2017), 2016.

444 Letey, J., Jury, W. A., Hadas, A., and Valoras, N.: Gas Diffusion as a Factor in Laboratory Incubation Studies on
445 Denitrification1, *J. Environ. Qual.*, 9, doi:10.2134/jeq1980.00472425000900020012x, 1980.

446 Maag, M. and Vinther, F. P.: Effect of temperature and water on gaseous emissions from soils treated with
447 animal slurry, *Soil Sci. Soc. Am. J.*, 63, 858–865, 1999.

448 Möller, K. and Müller, T.: Effects of anaerobic digestion on digestate nutrient availability and crop growth: A
449 review, *Eng. Life Sci.*, 12, 242–257, doi:10.1002/elsc.201100085, 2012.

450 Myhre, G., Shindell, D., Bréon, F. M., Collins, W., Fuglestvedt, J., Huang, J., Koch, D., Lamarque, J. F., Lee,
451 D., and Mendoza, B.: Anthropogenic and natural radiative forcing, in: *Climate Change 2013: The Physical
452 Science Basis.: Contribution of Working Group I to the Fifth Assessment Report of the Intergovernmental
453 Panel on Climate Change*, Stocker, T. F., Qin, D., Plattner, G. K., Tignor, M., Allen, S. K., Boschung, J.,
454 Nauels, A., Xia, Y., Bex, V., and Midgley, P. M. (Eds.), Cambridge University Press, Cambridge, United
455 Kingdom, New York, NY, USA, 659–740, 2013.

456 Nkoa, R.: Agricultural benefits and environmental risks of soil fertilization with anaerobic digestates: a review,
457 *Agron. Sustain. Dev.*, 1–20, doi:10.1007/s13593-013-0196-z, 2013.

458 Parkin, T. B. and Tiedje, J. M.: Application of a soil core method to investigate the effect of oxygen
459 concentration on denitrification, *Soil Biol. Biochem.*, 16, 331–334, doi:10.1016/0038-0717(84)90027-0,
460 1984.

461 Quakernack, R., Pacholski, A., Techow, A., Herrmann, A., Taube, F., and Kage, H.: Ammonia volatilization and
462 yield response of energy crops after fertilization with biogas residues in a coastal marsh of Northern
463 Germany, *Agric., Ecosyst. Environ.*, 160, 66–74, doi:10.1016/j.agee.2011.05.030, 2012.

464 R Core Team: R: A Language and Environment for Statistical Computing, Vienna, Austria, [https://www.R-
465 project.org](https://www.R-project.org) (last access: 10 August 2017), 2016.

466 Reddy, K. R., Rao, P. S. C., and Jessup, R. E.: The Effect of Carbon Mineralization on Denitrification Kinetics
467 in Mineral and Organic Soils I, *Soil Sci. Soc. Am. J.*, 46, 62–68,
468 doi:10.2136/sssaj1982.03615995004600010011x, 1982.

469 Scholefield, D., Hawkins, J. M. B., and Jackson, S. M.: Use of a flowing helium atmosphere incubation
470 technique to measure the effects of denitrification controls applied to intact cores of a clay soil, *Soil Biol.
471 Biochem.*, 29, 1337–1344, doi:10.1016/S0038-0717(97)00059-X, 1997.

472 Senbayram, M., Chen, R., Budai, A., Bakken, L., and Dittert, K.: N₂O emission and the N₂O/(N₂O + N₂) product
473 ratio of denitrification as controlled by available carbon substrates and nitrate concentrations, *Agric.,
474 Ecosyst. Environ.*, 147, 4–12, doi:10.1016/j.agee.2011.06.022, 2012.

475 Senbayram, M., Chen, R., Mühling, K. H., and Dittert, K.: Contribution of nitrification and denitrification to
476 nitrous oxide emissions from soils after application of biogas waste and other fertilizers, *Rapid Commun.
477 Mass Spectrom.*, 23, 2489–2498, doi:10.1002/rcm.4067, 2009.

478 Senbayram, M., Chen, R., Wienforth, B., Herrmann, A., Kage, H., Mühling, K. H., and Dittert, K.: Emission of
479 N₂O from Biogas Crop Production Systems in Northern Germany, *BioEnergy Res.*, 1–14,
480 doi:10.1007/s12155-014-9456-2, 2014.

481 Severin, M., Fuss, R., Well, R., Garlipp, F., and van den Weghe, H.: Soil, slurry and application effects on
482 greenhouse gas emissions, *Plant, Soil Environ.*, 61, 344–351, 2015.

483 Tiedje, J. M.: Ecology of denitrification and dissimilatory nitrate reduction to ammonium, in: *Biology of
484 anaerobic microorganisms*, Zehnder, A. J. B. (Ed.), John Wiley and Sons Inc, New York, 179–244, 1988.

485 Uchida, Y., Clough, T. J., Kelliher, F. M., and Sherlock, R. R.: Effects of aggregate size, soil compaction, and
486 bovine urine on N₂O emissions from a pasture soil, *Soil Biol. Biochem.*, 40, 924–931,
487 doi:10.1016/j.soilbio.2007.11.007, 2008.

488 Velthof, G. L. and Mosquera, J.: The impact of slurry application technique on nitrous oxide emission from
489 agricultural soils, *Agric., Ecosyst. Environ.*, 140, 298–308, doi:10.1016/j.agee.2010.12.017, 2011.

490 Venterea, R. T., Clough, T. J., Coulter, J. A., Breuillin-Sessoms, F., Wang, P., and Sadowsky, M. J.: Ammonium
491 sorption and ammonia inhibition of nitrite-oxidizing bacteria explain contrasting soil N₂O production, *Sci.*
492 *Rep.*, 5, 12153 EP -, 2015.

493 Wang, R., Feng, Q., Liao, T., Zheng, X., Butterbach-Bahl, K., Zhang, W., and Jin, C.: Effects of nitrate
494 concentration on the denitrification potential of a calcic cambisol and its fractions of N₂, N₂O and NO, *Plant*
495 *Soil*, 363, 175–189, doi:10.1007/s11104-012-1264-x, 2013.

496 Wang, R., Willibald, G., Feng, Q., Zheng, X., Liao, T., Brüggemann, N., and Butterbach-Bahl, K.: Measurement
497 of N₂, N₂O, NO, and CO₂ Emissions from Soil with the Gas-Flow-Soil-Core Technique, *Environ. Sci.*
498 *Technol.*, 45, 6066–6072, doi:10.1021/es1036578, 2011.

499 Webb, J., Pain, B., Bittman, S., and Morgan, J.: The impacts of manure application methods on emissions of
500 ammonia, nitrous oxide and on crop response—A review, *Agric., Ecosyst. Environ.*, 137, 39–46,
501 doi:10.1016/j.agee.2010.01.001, 2010.

502 West, S. G., Finch, J. F., and Curran, P. J.: Structural equation models with nonnormal variables: Problems and
503 remedies, in: *Structural equation modeling: Concepts, issues, and applications*, Hoyle, R. H. (Ed.), Sage,
504 Thousand Oaks, 56–75, 1995.

505 Wulf, S., Maeting, M., and Clemens, J.: Application technique and slurry co-fermentation effects on ammonia,
506 nitrous oxide, and methane emissions after spreading: II. Greenhouse gas emissions, *J. Environ. Qual.*, 31,
507 1795–1801, 2002.

508 Zhang, X., Davidson, E. A., Mauzerall, D. L., Searchinger, T. D., Dumas, P., and Shen, Y.: Managing nitrogen
509 for sustainable development, *Nature*, 528, 51–59, 2015.

510

511

512 **Table 1: The examined factors soil texture, water-filled pore space (WFPS), and amount (i.e., concentration) of nitrogen**
513 **(N) applied with biogas digestate (BD) with their respective levels applied in the present study, resulting in 18**
514 **treatments with three replicates each. The temperature was manipulated consecutively during the incubation.**

Factor [<i>n</i>]	Levels		
Soil texture [2]	loamy sand	clayey silt	
WFPS (%) [3]	35	55	75
BD-N (kg ha ⁻¹) [3]	0	160	320
Temperature (°C) [2]	2	15	

515

516 **Table 2: Characteristics of both soils. Texture and mean values with standard deviations (in brackets) for carbon (C, $n = 9$), nitrogen (N, $n = 9$), pH ($n = 3$), bulk density (BD, $n = 3$)**
 517 **and mineral N (NO_3^- and NH_4^+ , $n = 3$) of both soils in 0–10 cm depth after field sampling.**

Texture	C (mg g^{-1}) ^a	N (mg g^{-1}) ^a	pH ^b	Bulk density (g cm^{-3}) ^c	NO_3^- (mg kg^{-1}) ^d	NH_4^+ (mg kg^{-1}) ^d
Loamy sand	6.99 (0.29)	0.67 (0.05)	7.2 (0.1)	1.4 (0.0)	1.0 (0.2)	0.6 (0.3)
Clayey silt	10.77 (0.28)	1.19 (0.06)	7.2 (0.0)	1.5 (0.0)	1.8 (0.2)	0.3 (0.2)

518 ^a measured with analyser “Truspec CNS”, Leco Instruments GmbH, Germany, performed according to ISO 10694 (“elemental analysis”) for C and according to ISO 13878
 519 (“elemental analysis”) for N

520 ^b measured in H_2O with TitraMaster85, Radiometer Analytical SAS, France, performed according to VDLUFA Methodenbuch, Vol. 1, chap. 5.1.1

521 ^c measured on 250 cm^3 soil cores

522 ^d measured with analyser “CFA-SAN”, Skalar Analytical B.V., the Netherlands, performed according to ISO 14256

523 **Table 3: Chronological order of the incubated factor combinations. Two different factor combinations with their**
 524 **respective repetitions ($n = 3$) were placed together for each weekly incubation course (cf. Fig. 1). The factors were**
 525 **combined by (1) soil (loamy sand: LS, clayey silt: CS), (2) amount (kg) of applied N from digestate per ha and (3) WFPS**
 526 **(%).**

Week	Factor combination 1	Factor combination 2
1	LS - 0 N - 35%	LS - 0 N - 55%
2	LS - 0 N - 75%	LS - 160 N - 35%
3	LS - 160 N - 55%	LS - 160 N - 75%
4	LS - 320 N - 35%	LS - 320 N - 55%
5	LS - 320 N - 75%	CS - 0 N - 35%
6	CS - 0 N - 55%	CS - 0 N - 75%
7	CS - 160 N - 35%	CS - 160 N - 55%
8	CS - 160 N - 75%	CS - 320 N - 35%
9	CS - 320 N - 55%	CS - 320 N - 75%

527

528 **Table 4: Mean DOC values from soils, measured after incubation with standard deviations in brackets for the respective**
 529 **treatments differing in amount of applied biogas digestate (BD) and water-filled pore space (WFPS).**

kg digestate-N ha ⁻¹	WFPS (%)	mg DOC (kg soil) ⁻¹	
		Loamy sand	Clayey silt
0	35	41.4 (2.7)	18.9 (1.1)
	55	38.6 (3.1)	19.8 (1.4)
	75	43.7 (1.4)	19.0 (1.8)
160	35	197.4 (20.7)	n.a.
	55	190.5 (19.3)	68.3 (12.7)
	75	362.2 (40.0)	63.2 (9.6)
320	35	316.8 (25.3)	358.1 (26.3)
	55	312.5 (14.3)	94.8 (13.6)
	75	500.1 (33.4)	105.9 (14.8)

530 n.a.: data not available

531 **Table 5: ANOVA table (type 2, *p*-values calculated based on Satterthwaite's approximation) of the linear mixed effects models for estimated fluxes of N₂, N₂O, N₂/(N₂+N₂O) product**
 532 **ratio and CO₂ in aerobic He-O₂ atmosphere. Soil type, water-filled pore space (WFPS), amount of digestate, temperature, NO₃⁻ and DOC content of soil after incubation as well as**
 533 **fluxes of N₂O and CO₂ were set as possible independent variables. The individual soil rings were set as random effect (nested within the respective week and with the allowance for**
 534 **varying slopes for each day of measurements). The random effect was always significant.**

535

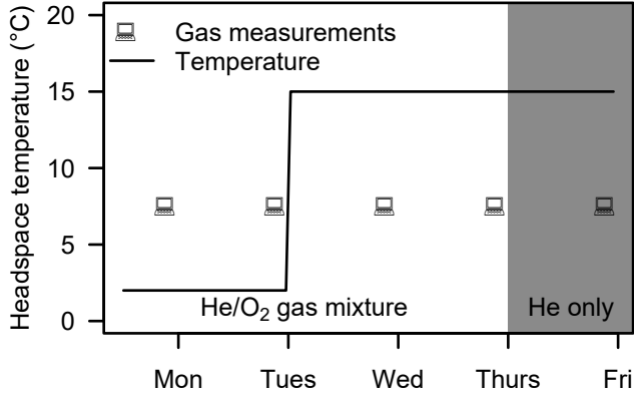
Fixed effects								
Response	Soil type	WFPS	Digestate amount	Temperature	NO ₃ ⁻ post	DOC post	N ₂ O flux	CO ₂ flux
N ₂	0.026	< 0.001	0.008	0.037	†	0.001	< 0.001	†
N ₂ O	†	< 0.001	< 0.001	< 0.001	†	< 0.001	*	< 0.001
N ₂ /(N ₂ +N ₂ O)	0.005	0.004	†	†	†	†	*	†
CO ₂	<0.001	†	<0.001	<0.001	†	0.007	†	*

536 † Variable eliminated during stepwise regression selection

537 * Variable was not included into original regression

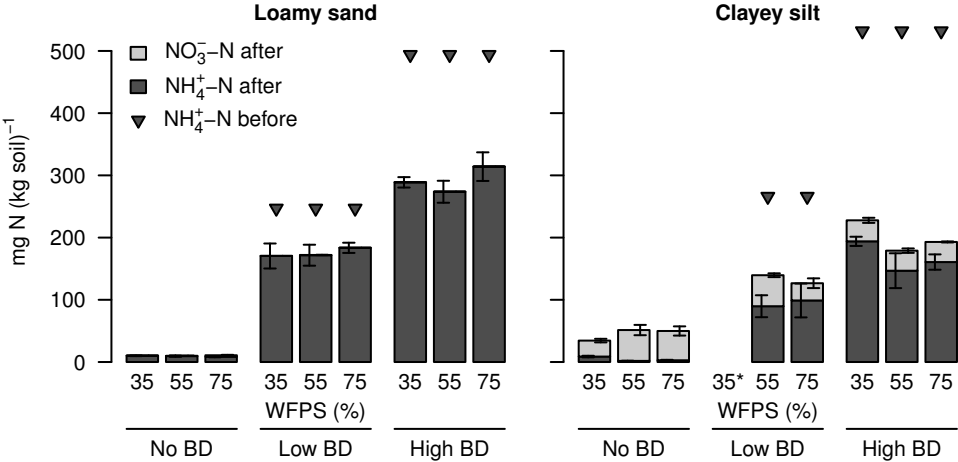
538 **Figure 1: Course of incubation and gas measurements with respect to atmosphere and temperature of the headspace**
539 **after two days of pre-incubation at 2 °C in He/O₂ gas mixture. Gas concentrations of the headspace were determined**
540 **on five consecutive days, i.e. Monday to Friday in the morning. After the first two measurement days, the headspace**
541 **temperature was increased from 2 to 15 °C. Additionally, after the fourth measurement day, the aerobic Helium/oxygen**
542 **gas mixture in the headspace was replaced by a pure Helium atmosphere.**

543

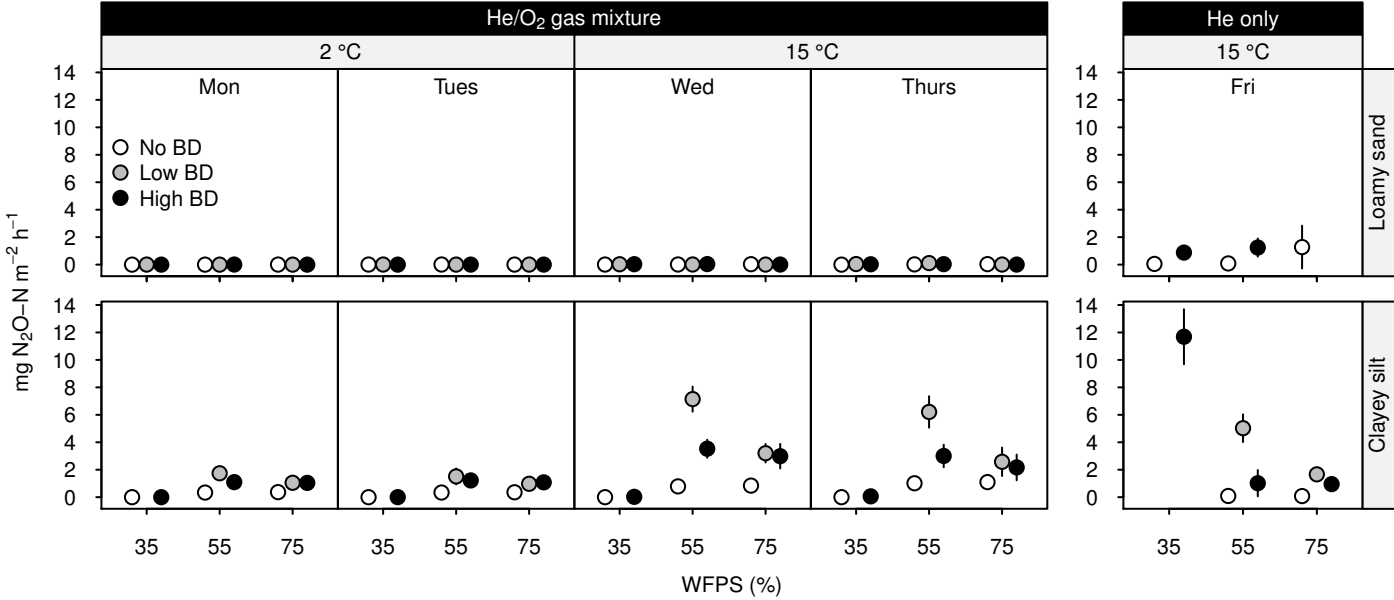


544 **Fig. 2: Ammonium and nitrate contents from loamy sand and clayey silt after incubation with different water-filled**
545 **pore spaces (WFPS, %) and amounts of digestate (0 mL per sample ring: 'No BD', 17.6 mL: 'Low BD' and 35.2 mL:**
546 **'High BD'). Error bars denote standard deviations. In general, the ammonium content increased with digestate**
547 **application with lower amounts detected in the clayey silt. Nitrate was found almost exclusively in the latter soil. For**
548 **comparison, calculated amounts of ammonium applied with biogas digestate are shown by triangles. One treatment (*)**
549 **was omitted from all analyses due to technical reasons.**

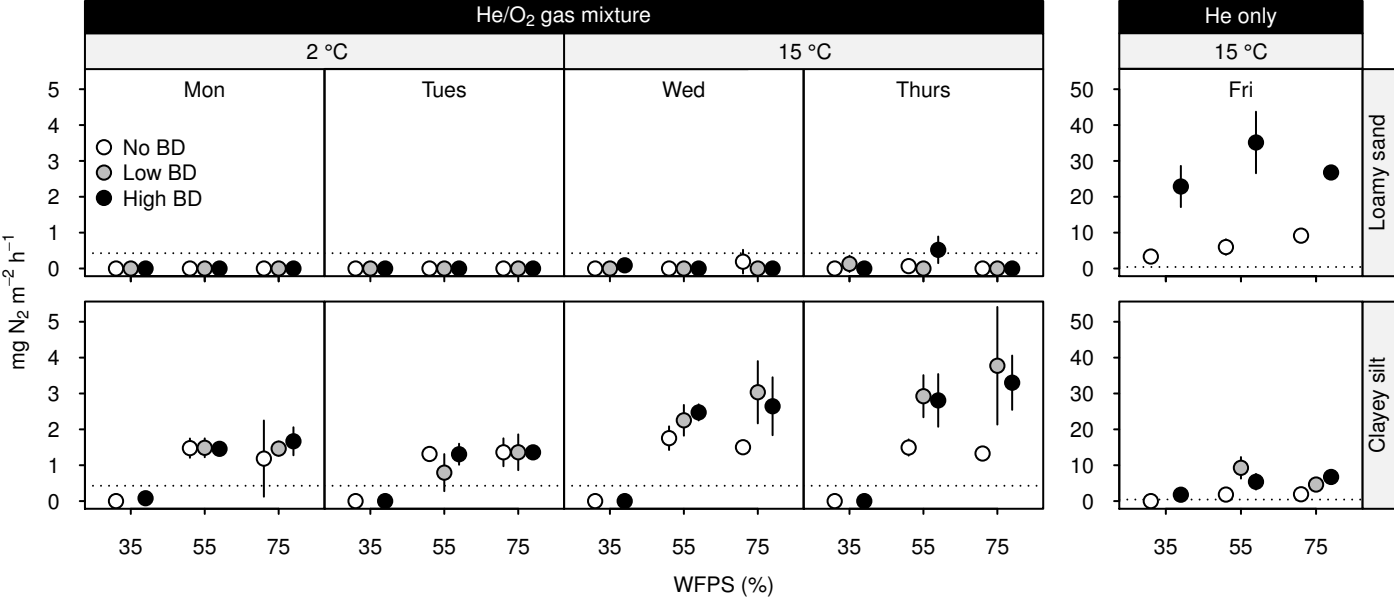
550



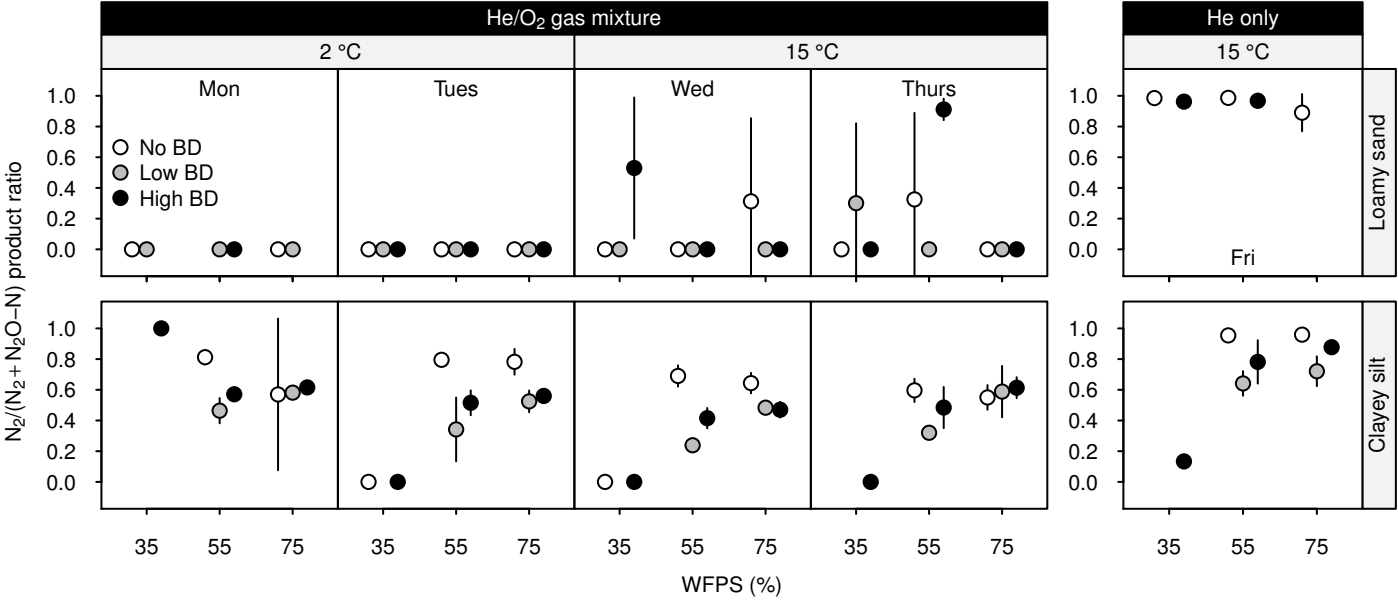
551 Fig. 3: Mean N₂O fluxes (mg N m⁻² h⁻¹) from a loamy sand and a clayey silt incubated under different water-filled pore
552 spaces (WFPS, %) with different amounts of digestate (0 mL per sample ring: 'No BD', 17.6 mL: 'Low BD' and 35.2
553 mL: 'High BD'). The first till the fourth day of the incubation were measured in an aerobic He-O₂ headspace (with two
554 days at 2 °C followed by another two days at 15 °C) while on the fifth day measurements were conducted in an
555 anaerobic headspace with pure He (at 15 °C). Error bars show standard deviations; if bars are not visible, they are
556 smaller than the symbols of the means. Under aerobic atmosphere, N₂O fluxes from loamy sand were negligible, while
557 fluxes from clayey silt showed an increase with temperature, especially with higher WFPS and intermediate amounts
558 of digestate. Under anaerobic atmosphere, mean fluxes from loamy sand increased slightly, but significantly (Tukey's
559 HSD, *p* < 0.05). The fluxes from clayey silt showed no significant differences (Tukey's HSD, *p* < 0.05) compared to the
560 day before, with the exception of 35% WFPS, where mean flux increased strongly in the treatment with 320 kg digestate-
561 N ha⁻¹.



562 Fig. 4: Mean N₂ fluxes (mg m⁻² h⁻¹) from a loamy sand and a clayey silt incubated under different water-filled pore
563 spaces (WFPS, %) with different amounts of digestate (0 mL per sample ring: 'No BD', 17.6 mL: 'Low BD' and 35.2
564 mL: 'High BD'). The first till the fourth day of the incubation were measured in an aerobic He-O₂ headspace (with two
565 days at 2 °C followed by another two days at 15 °C) while on the fifth day measurements were conducted in an
566 anaerobic headspace with pure He (at 15 °C). Error bars show standard deviations; if bars are not visible, they are
567 smaller than the symbols of the means. The dotted horizontal lines depict the average blank value; single flux rates
568 lower than the respective blank value were set zero. Under aerobic atmosphere, N₂ fluxes from loamy sand were zero or
569 rather negligible, while fluxes from clayey silt show a distinct increase with WFPS and higher fluxes at 15 °C. Under
570 anaerobic atmosphere, mean fluxes from loamy sand increased by orders of magnitude, while the fluxes from clayey
571 silt increased as well, but more gently compared to the sand.

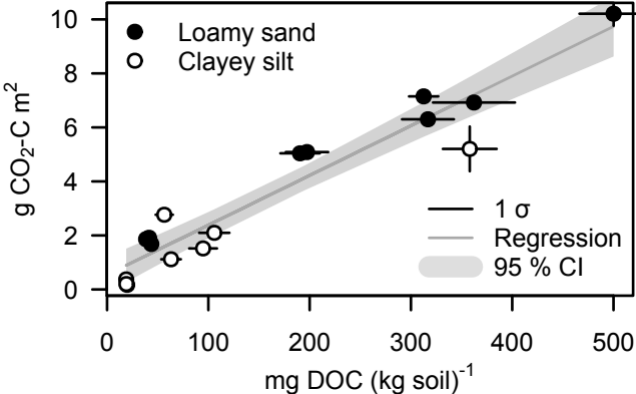


572 **Fig. 5: Mean $N_2/(N_2 + N_2O-N)$ product ratio from a loamy sand and a clayey silt incubated under different water-filled**
573 **pore spaces (WFPS, %) with different amounts of digestate (0 mL per sample ring: ‘No BD’, 17.6 mL: ‘Low BD’ and**
574 **35.2 mL: ‘High BD’). The first till the fourth day of the incubation were measured in an aerobic He-O₂ headspace (with**
575 **two days at 2 °C followed by another two days at 15 °C) while on the fifth day measurements where conducted in an**
576 **anaerobic headspace with pure He (at 15 °C). Error bars show standard deviations; if bars are not visible, they are**
577 **smaller than the symbols of the means. For the loamy sand, there was a clear distinction of the ratios between aerobic**
578 **and anaerobic atmospheres: while the ratios tended to 0 in the former, they tended to 1 in the latter, irrespectively of**
579 **temperature or amount of digestate. For the clayey silt, ratios increased with WFPS and were highest from the**
580 **unamended treatments under both the aerobic and the anaerobic atmospheres.**

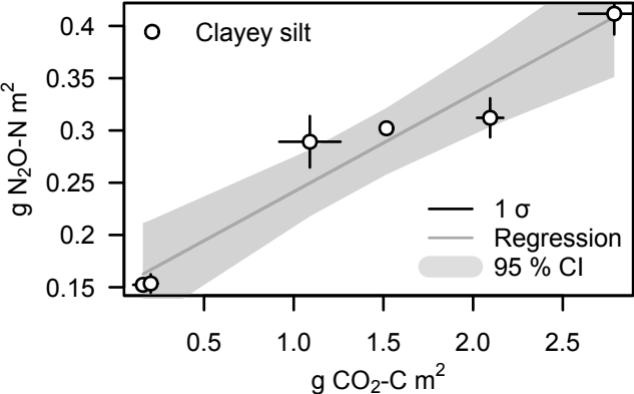


581 **Fig. 6: Regression between DOC (mg per 100 g soil) measured after the incubation and the respective cumulated CO₂**
582 **emissions (g C m⁻²) during the period of aerobic headspace with their standard deviations and confidence interval**
583 **(95%). If error bars are not visible, they are smaller than the symbols of the means. Both soils showed increasing**
584 **emissions with increasing soil DOC contents as well a good regression fit ($R^2 = 0.91, p < 0.001$).**

585



586 **Fig. 7: Regression between cumulated CO₂ emissions (g C m⁻²) and the respective cumulated N₂O + N₂ emissions (g N**
587 **m⁻²) from the clayey silt with WFPS > 35 % during the period of aerobic headspace with their standard deviations and**
588 **confidence interval (95%). If error bars are not visible, they are smaller than the symbols of the means. The proportional**
589 **increase of CO₂ and the N gas species shows a good regression fit of $R^2 = 0.93$, ($p = 0.001$).**



590 **Table A1: Mean CO₂-C fluxes with standard deviations in mg m⁻² h⁻¹ from the loamy sand and the clayey silt, treated**
591 **with different water-filled pore spaces (WFPS, %), amounts of digestate (kg N ha⁻¹) as well as different temperature**
592 **regimes (°C) under aerobic (He-O₂) and anaerobic (He) atmosphere. Column 'Day' denotes the consecutive measuring**
593 **days of the respective incubation cycle. Different letters after fluxes indicate significant differences (Tukey's HSD, *p* <**
594 **0.05) within each soil and measuring day. Zeros as last digits were omitted.**

Day	Atmosphere	Temperature (°C)	WFPS (%)	kg N ha ⁻¹	mg CO ₂ -C m ⁻² h ⁻¹	
					Loamy sand	Clayey silt
1	He-O ₂	2	35	0	6.8 ± 2.4 cd	0 ± 0 c
1	He-O ₂	2	35	160	22 ± 3.5 bcd	NA
1	He-O ₂	2	35	320	23.3 ± 9.3 bc	22.8 ± 2.8 ab
1	He-O ₂	2	55	0	6 ± 0.7 d	4.6 ± 7.9 bc
1	He-O ₂	2	55	160	34.4 ± 3.1 b	34.5 ± 11.6 a
1	He-O ₂	2	55	320	28 ± 3.2 b	15.9 ± 3.4 abc
1	He-O ₂	2	75	0	9.4 ± 1.4 cd	0 ± 0 c
1	He-O ₂	2	75	160	37.5 ± 6 b	15.5 ± 12.1 abc
1	He-O ₂	2	75	320	68.3 ± 12.1 a	24.5 ± 2.7 a
2	He-O ₂	2	35	0	9.8 ± 3.5 c	1.3 ± 1.4 b
2	He-O ₂	2	35	160	23 ± 3.9 bc	NA
2	He-O ₂	2	35	320	30.9 ± 2.2 b	22.2 ± 2.4 a
2	He-O ₂	2	55	0	8.7 ± 1.5 c	0.6 ± 1 b
2	He-O ₂	2	55	160	33.4 ± 0.9 b	27.6 ± 12.3 a
2	He-O ₂	2	55	320	35.9 ± 2.7 b	14.4 ± 1.9 ab
2	He-O ₂	2	75	0	8.3 ± 1.5 c	0 ± 0 b
2	He-O ₂	2	75	160	31.9 ± 3 b	13 ± 9.3 ab
2	He-O ₂	2	75	320	57.6 ± 14.8 a	18.3 ± 4 a
3	He-O ₂	15	35	0	42.5 ± 4.5 c	6.7 ± 0.7 b
3	He-O ₂	15	35	160	114.3 ± 12.2 b	NA
3	He-O ₂	15	35	320	149.5 ± 9.4 b	130.9 ± 105 a
3	He-O ₂	15	55	0	41.3 ± 3.5 c	3.2 ± 0.4 b
3	He-O ₂	15	55	160	108.7 ± 10.1 b	57.8 ± 12.2 bc
3	He-O ₂	15	55	320	162.1 ± 9.6 b	26.8 ± 0.7 bc
3	He-O ₂	15	75	0	44.1 ± 9.8 c	3.2 ± 0.7 b
3	He-O ₂	15	75	160	150.4 ± 19 b	26.4 ± 11.8 bc
3	He-O ₂	15	75	320	249.7 ± 53.5 a	35.3 ± 6 bc
4	He-O ₂	15	35	0	48.7 ± 6 c	15.1 ± 4.9 cd
4	He-O ₂	15	35	160	114.3 ± 6.4 b	NA
4	He-O ₂	15	35	320	156.9 ± 15.4 a	65.7 ± 2.2 a
4	He-O ₂	15	55	0	48 ± 3.4 c	4.2 ± 0.2 d
4	He-O ₂	15	55	160	109 ± 14.4 b	51.2 ± 15.1 ab

4	He-O ₂	15	55	320	177.7 ± 7.5 a	26.6 ± 2.3 cd
4	He-O ₂	15	75	0	34 ± 7.8 c	6.7 ± 4 d
4	He-O ₂	15	75	160	168.7 ± 0.4 a	22.1 ± 14.8 cd
4	He-O ₂	15	75	320	166.3 ± 23.1 a	34.1 ± 5.7 bc
5	He	15	35	0	11.2 ± 0.6 d	NA
5	He	15	35	160	54.8 ± 9.3 c	NA
5	He	15	35	320	149.3 ± 3.9 a	45.8 ± 2.1 a
5	He	15	55	0	13.6 ± 1.9 d	3.4 ± 0.6 c
5	He	15	55	160	55.2 ± 4.4 bc	32 ± 11.4 ab
5	He	15	55	320	164.5 ± 3.5 a	15.2 ± 10.7 bc
5	He	15	75	0	20.9 ± 2.3 d	3.6 ± 0.1 c
5	He	15	75	160	75 ± 7.3 b	20.6 ± 8.5 bc
5	He	15	75	320	NA	26.1 ± 2.6 ab

595

596 **Table A2: Mean N₂O-N fluxes with standard deviations in mg m⁻² h⁻¹ from the loamy sand and the clayey silt, treated**
597 **with different water-filled pore spaces (WFPS, %), amounts of digestate (kg N ha⁻¹) as well as different temperature**
598 **regimes (°C) under aerobic (He-O₂) and anaerobic (He) atmosphere. Column 'Day' denotes the consecutive measuring**
599 **days of the respective incubation cycle. Different letters after fluxes indicate significant differences (Tukey's HSD, *p* <**
600 **0.05) within each soil and measuring day. Zeros as last digits were omitted.**

Day	Atmosphere	Temperature (°C)	WFPS (%)	kg N ha ⁻¹	mg N ₂ O-N m ⁻² h ⁻¹	
					Loamy sand	Clayey silt
1	He-O ₂	2	35	0	0 ± 0	0 ± 0 c
1	He-O ₂	2	35	160	0 ± 0	NA
1	He-O ₂	2	35	320	0 ± 0	0 ± 0 c
1	He-O ₂	2	55	0	0 ± 0	0.3 ± 0.1 c
1	He-O ₂	2	55	160	0 ± 0	1.7 ± 0.4 a
1	He-O ₂	2	55	320	0 ± 0	1.1 ± 0.1 b
1	He-O ₂	2	75	0	0 ± 0	0.4 ± 0.1 c
1	He-O ₂	2	75	160	0 ± 0	1 ± 0.1 b
1	He-O ₂	2	75	320	0 ± 0	1 ± 0.2 b
2	He-O ₂	2	35	0	0 ± 0	0 ± 0 d
2	He-O ₂	2	35	160	0 ± 0	NA
2	He-O ₂	2	35	320	0 ± 0	0 ± 0 cd
2	He-O ₂	2	55	0	0 ± 0	0.3 ± 0.1 bc
2	He-O ₂	2	55	160	0 ± 0	1.5 ± 0.6 a
2	He-O ₂	2	55	320	0 ± 0	1.2 ± 0.2 a
2	He-O ₂	2	75	0	0 ± 0	0.4 ± 0.1 bc
2	He-O ₂	2	75	160	0 ± 0	1 ± 0.1 ab
2	He-O ₂	2	75	320	0 ± 0	1.1 ± 0.2 a
3	He-O ₂	15	35	0	0 ± 0 cd	0 ± 0 c
3	He-O ₂	15	35	160	0 ± 0 abc	NA
3	He-O ₂	15	35	320	0 ± 0 ab	0 ± 0 c
3	He-O ₂	15	55	0	0 ± 0 bcd	0.8 ± 0.2 c
3	He-O ₂	15	55	160	0 ± 0 bcd	7.1 ± 0.9 a
3	He-O ₂	15	55	320	0 ± 0 a	3.5 ± 0.7 b
3	He-O ₂	15	75	0	0 ± 0 ab	0.8 ± 0.2 c
3	He-O ₂	15	75	160	0 ± 0 d	3.2 ± 0.7 b
3	He-O ₂	15	75	320	0 ± 0 cd	3 ± 0.9 b
4	He-O ₂	15	35	0	0 ± 0 b	0 ± 0 c
4	He-O ₂	15	35	160	0 ± 0 ab	NA
4	He-O ₂	15	35	320	0 ± 0 ab	0.1 ± 0.1 c
4	He-O ₂	15	55	0	0 ± 0 b	1 ± 0.2 bc
4	He-O ₂	15	55	160	0.1 ± 0.1 a	6.2 ± 1.1 a

4	He-O ₂	15	55	320	0 ± 0 ab	3 ± 0.8 b
4	He-O ₂	15	75	0	0 ± 0 ab	1.1 ± 0.3 bc
4	He-O ₂	15	75	160	0 ± 0 b	2.6 ± 1 b
4	He-O ₂	15	75	320	0 ± 0 b	2.2 ± 0.9 b
5	He	15	35	0	0.1 ± 0	NA
5	He	15	35	160	NA	NA
5	He	15	35	320	0.9 ± 0.1	11.7 ± 2 a
5	He	15	55	0	0.1 ± 0	0.1 ± 0 c
5	He	15	55	160	NA	5 ± 1 b
5	He	15	55	320	1.2 ± 0.7	1.4 ± 0.8 c
5	He	15	75	0	1.3 ± 1.6	0.1 ± 0 c
5	He	15	75	160	NA	1.7 ± 0.3 c
5	He	15	75	320	NA	1 ± 0.3 c

601

602 **Table A3: Mean N₂ fluxes with standard deviations in mg m⁻² h⁻¹ from the loamy sand and the clayey silt, treated with**
603 **different water-filled pore spaces (WFPS, %), amounts of digestate (kg N ha⁻¹) as well as different temperature regimes**
604 **(°C) under aerobic (He-O₂) and anaerobic (He) atmosphere. Column 'Day' denotes the consecutive measuring days of**
605 **the respective incubation cycle. Different letters after fluxes indicate significant differences (Tukey's HSD, *p* < 0.05)**
606 **within each soil and measuring day. Zeros as last digits were omitted.**

	Atmosphere	Temperature (°C)	WFPS (%)	kg N ha ⁻¹	mg N ₂ m ⁻² h ⁻¹	
					Loamy sand	Clayey silt
1	He-O ₂	2	35	0	0 ± 0	0 ± 0 bc
1	He-O ₂	2	35	160	0 ± 0	NA
1	He-O ₂	2	35	320	0 ± 0	0.1 ± 0.1 bc
1	He-O ₂	2	55	0	0 ± 0	1.5 ± 0.3 a
1	He-O ₂	2	55	160	0 ± 0	1.5 ± 0.3 a
1	He-O ₂	2	55	320	0 ± 0	1.5 ± 0 a
1	He-O ₂	2	75	0	0 ± 0	1.2 ± 1.1 a
1	He-O ₂	2	75	160	0 ± 0	1.5 ± 0.2 a
1	He-O ₂	2	75	320	0 ± 0	1.7 ± 0.4 a
2	He-O ₂	2	35	0	0 ± 0	0 ± 0 c
2	He-O ₂	2	35	160	0 ± 0	NA
2	He-O ₂	2	35	320	0 ± 0	0 ± 0 c
2	He-O ₂	2	55	0	0 ± 0	1.3 ± 0.1 a
2	He-O ₂	2	55	160	0 ± 0	0.8 ± 0.5 b
2	He-O ₂	2	55	320	0 ± 0	1.3 ± 0.3 a
2	He-O ₂	2	75	0	0 ± 0	1.4 ± 0.4 a
2	He-O ₂	2	75	160	0 ± 0	1.4 ± 0.5 a
2	He-O ₂	2	75	320	0 ± 0	1.4 ± 0.1 a
3	He-O ₂	15	35	0	0 ± 0 b	0 ± 0 e
3	He-O ₂	15	35	160	0 ± 0 b	NA
3	He-O ₂	15	35	320	0.1 ± 0.1 ab	0 ± 0 e
3	He-O ₂	15	55	0	0 ± 0 b	1.8 ± 0.3 cd
3	He-O ₂	15	55	160	0 ± 0 b	2.3 ± 0.4 bc
3	He-O ₂	15	55	320	0 ± 0 b	2.5 ± 0.2 ab
3	He-O ₂	15	75	0	0.2 ± 0.3 a	1.5 ± 0.2 d
3	He-O ₂	15	75	160	0 ± 0 b	3 ± 0.9 a
3	He-O ₂	15	75	320	0 ± 0 b	2.6 ± 0.8 ab
4	He-O ₂	15	35	0	0 ± 0 b	0 ± 0 c
4	He-O ₂	15	35	160	0.1 ± 0.2 b	NA
4	He-O ₂	15	35	320	0 ± 0 b	0 ± 0 c
4	He-O ₂	15	55	0	0.1 ± 0.1 b	1.5 ± 0.2 b
4	He-O ₂	15	55	160	0 ± 0 b	2.9 ± 0.6 a

4	He-O ₂	15	55	320	0.5 ± 0.4 a	2.8 ± 0.7 a
4	He-O ₂	15	75	0	0 ± 0 b	1.3 ± 0.2 bc
4	He-O ₂	15	75	160	0 ± 0 b	3.8 ± 1.6 a
4	He-O ₂	15	75	320	0 ± 0 b	3.3 ± 0.8 a
5	He	15	35	0	3.3 ± 0.4 d	0 ± 0 c
5	He	15	35	160	NA	NA
5	He	15	35	320	22.9 ± 5.7 b	1.8 ± 0.1 c
5	He	15	55	0	6 ± 2.2 cd	1.8 ± 0.2
5	He	15	55	160	NA	9.5 ± 2.7 a
5	He	15	55	320	35.1 ± 8.6 a	5.1 ± 1.8 bc
5	He	15	75	0	9.2 ± 0.4 c	1.9 ± 0.1 c
5	He	15	75	160	NA	4.8 ± 1.6 bc
5	He	15	75	320	26.8 ± 1.1 b	6.7 ± 0.8 b

607